Optimal Wind Turbine Yaw Control Supported with Very Short-term Wind Predictions

Nikola Hure*, Robi Turnar*, Mario Vašak*, Goran Benčić†
*University of Zagreb, Faculty of Electrical Engineering and Computing
Department of Control and Computer Engineering
†KONČAR - Power Plant and Electric Traction Engineering Inc.
nikola.hure@fer.hr, robi.turnar@fer.hr, mario.vasak@fer.hr, goran.bencic@koncar-ket.hr

***Abstract*—This paper is focused on design of a wind turbine optimal yaw control system based on very short-term wind predictions. The optimal controller performance is evaluated with respect to the power production maximisation and structural loads minimisation goals that are joined together in a single performance function expressing the profit of the wind turbine control system operation. Designed optimal yaw controller performance is compared to the baseline controller in the professional aeroelastic simulator GH Bladed. The results show effectiveness of the developed optimal wind turbine yaw angle controller, since it demonstrated damage equivalent loads reduction and power production increase.**

***Index Terms*—Wind Turbine, Yaw Control, Wind Prediction, Power Production, Structural Loads Mitigation, Optimal Control**

I. Introduction

Wind energy has become fastest growing renewable source considering the installed capacity per year [1]. Unlike the other alternative sources, wind power industry has reached a mature commercial phase. Nevertheless, wind turbines are continuously increasing size and nominal power capacity in order to achieve more competitive cost of energy compared to conventional sources.

Among the large wind turbines, variable-speed and pitch controlled turbines are predominant. The efficiency that they achieve depends mostly on the control algorithm used for turbine operation. Besides the power production efficiency, in order to make the wind turbine profitable the controller has to take care of the structural loads mitigation. Only considering both of the aforementioned control objectives can lead to optimal lifetime and production combination that will lead to maximum profit. It is high intermittence of wind power that make this task a challenge.

Compared to the number of papers dealing with the variable-speed variable-pitch wind turbine control, for the best of our knowledge, there is only a few of them dealing with the yaw control problem, e.g. [2], [3]. The simplest approach utilizes measurements of the wind direction from a wind vane and a classic PD or PID controller to steer the nacelle into wind, with some allowable steady-state regulation error [4]. Similarly, authors in [5], [2] use a fuzzy controller instead of the classic linear controller and show improvement of the control system performance. All those approaches have large sensitivity on the wind vane measurement error. Approaches which circumvent the wind vane measurement use the measurement of the produced electrical power instead, which is then used to find its maximum employing the hill climbing method with nacelle orientation as the perturbation variable [3], [6], [7]. Nevertheless, there is no paper dealing with the optimal yaw angle control incorporating short-term wind predictions [8], what makes it a main contribution of the research presented in this paper.

The rest of the paper is organized as follows. In the second section, common wind turbine control structure including wind turbine rotor and yaw control systems is presented. In Section III, compendious introduction to the structural loads analysis is presented. In the following section, optimal yaw control problem incorporating power production and fatigue loading is formulated and means for the optimal solution derivation is described. Section V presents validation results of the designed optimal controller performance compared to the baseline control system.

II. Wind turbine control system

Modern variable-speed variable-pitch wind turbines operate in two control regions. First region is so called low wind speed region where all available wind power is captured by tracking the optimal turbine rotational speed. In second, so called high wind speed region, the generated output power is maintained constant controlling the rotor-effective aerodynamic torque. Described control strategies are achieved with two distinct control loops, torque control loop and blade pitch control loop, as shown in Fig. 1.

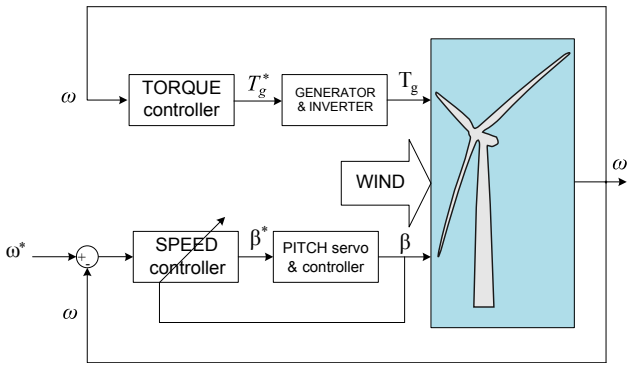

Fig. 1. Wind turbine rotor control loops

Wind turbine that is considered in this paper is upwind type and has a nominal power of 1 [MW]. It has a nominal wind speed of 12 [m/s] and a nominal rotor speed of 27 [rpm]. The generator torque control and blade pitch control loop constitute together a turbine regulation and control the mechanical power that is extracted from the rotor-effective wind speed, while there is a need of additional control loop in order to overcome the problem of the wind direction variability.

A. *Wind turbine yaw control*

To maximise overall power output, rotor axis must be aligned with wind direction. It is achieved by rotating the nacelle around the vertical tower axis. Coordinate system with denoted referent directions of variables used for the wind turbine yaw control problem is shown in Fig. 2.

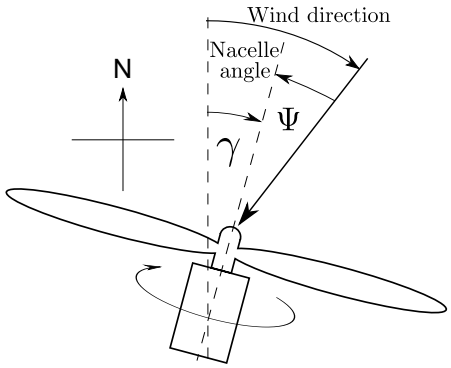

Fig. 2. Wind turbine yaw misalignment

Yaw misalignment affects the production as well as the structural loads. Static characteristics of the generated mechanical power on the wind turbine shaft with respect to mean wind speed value and yaw angle misalignment is shown in Fig. 3. It can be observed that increase of yaw misalignment results with a drop of generated power.

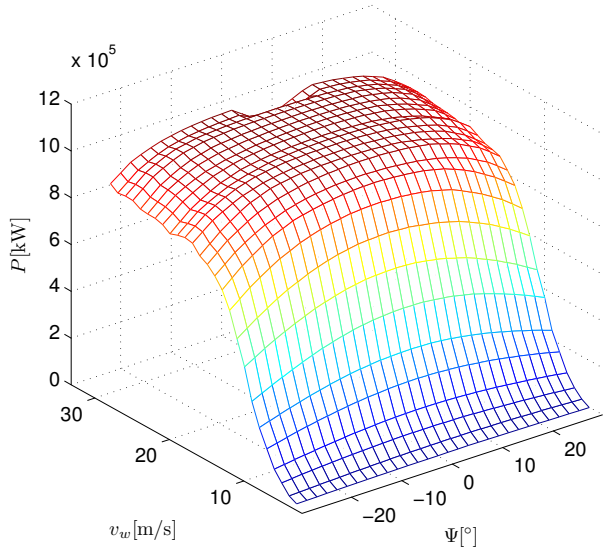

Fig. 3. Output power in case of the yaw misalignment

Baseline yaw control system, which is utilized for the control system validation in this paper, operates with the presumption of persistent wind prediction model: averaged wind direction in the last discrete-time period of the yaw control system is considered as the best wind angle estimate and as such, it is used as the nacelle angle position reference for the current discrete-time control period. Rotational speed of the yaw manoeuvre is limited to low enough value that prevents manifestation of gyroscopic forces which may easily endanger the wind turbine structure keeping in mind dimensions of the wind turbine rotor.

Mechanical part of the considered yaw mechanism consists of four motors with a gearbox connected to a tower gear rim (Fig. 4). Specifically, brakes are positioned on the motor side of the mechanism which results with a lower needed torque for the brakes. On the other side, loads experienced in the yaw axis are acting continuously on the yaw mechanism, thus increasing the fatigue of all elements in that chain.

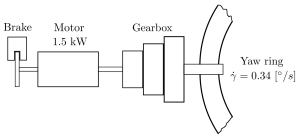

Fig. 4. Wind turbine yaw mechanism elements

Yawing motors are engaged by soft-starters that allow gradual start of the yaw manoeuvre. The initial transient approximately lasts half of a second, after which motors and nacelle achieve their nominal speed.

This simple yaw control does not consider the influence of the yaw misalignment on the structural loads of the wind turbine, neither it exploits information of the wind prediction. Considering these two elements raises the opportunity to develop a better yawing algorithm that will cover all important aspects of the wind turbine optimal exploitation.

In this paper, the optimal controller is designed to operate

with incorporated information about the wind speed and wind angle predictions. The topic of acquiring the respective predictions is not considered in this paper, and for additional information the reader is referred to e.g. [8], [9] and [10].

III. Short Introduction to Structural Loads Analysis

Structural loads that manifest on the wind turbine are mostly the result of a varying wind characteristics. Two places that are mostly considered, from control system point of view, are the blade root and the tower top. The oscillating nature of manifested loads due to three blades rotating in the variable wind field requires that appropriate method is used for the calculation of the experienced structural damage.

Fatigue failure is the result of the accumulation of damage due to fluctuating loads. These fluctuating loads are broken down into individual hysteresis cycles, employing the rainflow counting algorithm. Each cycle in these loads is characterized by its mean and range value. It is assumed that damage accumulates lineary with each of these cycles according to the Miner's rule [11]. Total damage from all cycles is then equal to

$$D = \sum_i \frac{n_i}{N_i}, \tag{1}$$

where N_i (2) denotes the number of cycles to failure and models the relationship between load range and cycles to failure (S-N curve), n_i is the cycle count for individual hysteresis cycle i. The number of cycles N_i is defined with

$$N_i = \left(\frac{L^{ULT} - |L^{MF}|}{\frac{1}{2} L_i^{RF}} \right)^m, \tag{2}$$

where L^{ULT} is the ultimate design load and m is the Wöhler exponent, both of them are specific for the component material that is under consideration. Typical value of Wöhler exponent for steel is 4 (tower) and 10 for composite materials (blades). L_i^{RF} (3) is the cycle's load range about a fixed mean value L^{MF}, with so called Goodman's correction. Since the actual load cycles occur over a spectrum of mean loads L_i^M, cycle load ranges L_i^R are corrected as if each cycle occurred about a fixed mean load L^{MF}. The cycle's load range is determined from

$$L_i^{RF} = L_i^R \left(\frac{L^{ULT} - |L^{MF}|}{L^{ULT} - |L_i^M|} \right). \tag{3}$$

The most widely used measure for the load cases comparison is damage equivalent load (DEL). The main goal is to calculate constant amplitude fatigue load that occurs at a fixed mean load and frequency and produces the damage equivalent to the variable spectrum loads (4),

$$D = \sum_i \frac{n_i}{N_i} = \frac{n^{eq}}{N^{eq}}. \tag{4}$$

Total equivalent fatigue count n^{eq} (5) is calculated from selected DEL frequency and elapsed time,

$$n^{eq} = f^{eq} T. \tag{5}$$

N^{eq} (6) corresponds to the equivalent number of cycles until failure which is obtained with substituting L_i^{RF} with DEL,

$$N^{eq} = \left(\frac{L^{ULT} - |L^{MF}|}{\frac{1}{2} DEL} \right)^m. \tag{6}$$

Solving equation (4) for DEL yields

$$DEL = \left(\frac{\sum_i (n_i (L_i^{RF})^m)}{n^{eq}} \right)^{\frac{1}{m}}. \tag{7}$$

Aformentioned calculations are carried out in MLife, MATLAB-based tool used for post-processing of the results from wind turbine tests [11]. In this paper, damages to the wind turbine components are calculated from the simulation data to obtain the performance function terms for the optimal controller synthesis, while DELs are used to validate the performance of the optimal yaw controller compared to the baseline yaw control system.

IV. Optimal Wind Turbine Yaw Controller Synthesis

The task of the high level optimal controller is to derive the cost-optimal reference for the low level yaw control system in each discrete-time step T_d. Since the wind speed and wind inflow angle predictions, as well as the actuator limits have to be considered by the controller, model predictive control [12] paradigm is used for the controller design.

In model predictive control approach, open loop dynamics of the system states and system constraints, as well as the defined performance measure $J(x_0, U, D)$, where x_0 is the initial system state, $U = [u_0, u_1, \ldots, u_{N-1}]$ is the control input prediction and D is the predicted disturbance sequence, are used to pose the control problem in the constrained optimization form. Various approaches are developed to solve arising optimization problem, and they are mostly defined by the structure of the controlled system and process requirements [13], [14], [15]. Once computed, the optimal control policy $U^* = [u_0^*, u_1^*, \ldots u_{N-1}^*]$, where N is the prediction horizon, is applied to the system in the receding horizon manner, i.e. the first control input u_0^* is applied to the plant whereas the next control input is obtained repeating the optimization problem in the next discrete-time step with refreshed system state and disturbance prediction.

For the considered high level control, observed dynamics of the wind turbine yaw comply to the following state-space equation,

$$\gamma_{k+1} = \gamma_k + \omega_y T_d u_k, \tag{8}$$

where γ is the yaw angle of the nacelle, ω_y is the fixed rotational speed of the nacelle, T_d is the sampling time of the system and $u_k \in (-1, 1)$ is the applied high level control input. Discretisation time of the high level yaw control system as well as the wind predictions is equal to $T_d = 60$ $[s]$.

A. Optimal yaw control problem formulation

It has been noted that wind turbine yaw misalignment has great influence on the power production as well as the fatigue loading of the wind turbine components. Both are included in the optimization problem whereas for their common measure in the performance function is used profit. Accordingly, chosen optimal yaw control formulation is the following

$$U^* = \arg\max_{U} \sum_{k=0}^{N-1} \{c_{el} E_{k,el} - \sum_{j} c_j D_{k,j}\},$$
$$\text{s.t.} \quad \left.\begin{array}{c} u_k \in (-1,1) \\ -4\pi \leq \gamma_{k+1} \leq 4\pi \end{array}\right\} \forall k \in \{0,1,\ldots,N-1\}. \tag{9}$$

In (9), c_{el} denotes the price of the electrical energy generated by the wind turbine and c_j is the price of the damage $D_{k,j}$ experienced by the wind turbine component j in the discrete-time step k. Price of the damage can be calculated to include price of the substitute as well as the commissioning and maintenance costs for the respective wind turbine components due to experienced damage.

Damage quantities of the considered wind turbine components are identified using the extensive simulation data of the power production loading with respect to the whole map of different wind speed conditions and operating states of the yaw control system.

B. Static performance function identification

For each field of wind speed ranging from 3 to 30 [m/s] with 1 [m/s] discrete step, and yaw misalignment starting from -45 [°] to 45 [°] with discrete step equal to 5 [°], 10 wind fields with different seed and duration equal to the discretisation time of the controller T_d are generated. The wind turbulence properties are set according to the IEC ed. 3 norm [16] of the normal turbulence model with A category of the wind turbulence that designates higher turbulence characteristics. For each wind field, power production simulation tests are performed with all possible operating states of the yaw control system:

1) fixed nacelle,
2) full-speed clockwise nacelle rotation,
3) full-speed counter-clockwise nacelle rotation.

Obtained simulation results are used to analyse damage rates experienced in different points of the wind turbine structure. Specifically, analysis of the obtained blade root and yaw bearing loads resulted with three most significant ones which are selected for further consideration. These loads with corresponding coordinate systems are shown in Fig. 5. Selection is based on the peak values of the loadings and the fact that they generate the most of the fatigue during the power production loading.

Tower loads are also observed as the yaw bearing system loads which are far more appropriate to be used in the perspective of the yaw control system synthesis. Therefore, instead of tower loads, in the remainder of this paper we use $M_{Y,yaw}$ and $M_{Z,yaw}$ instead of $M_{Y,tower}$ and $M_{Z,tower}$, respectively. Expected damage rates due to the considered loads in the case of fixed yaw nacelle are shown in Figs. 6, 7 and 8. These results are exploited in order to form a cummulative performance function,

$$F_i(v_w, \Psi) = \{c_{el} P_{el,i} - c_{M_{Y,yaw}} DR_{M_{Y,yaw},i} \ldots$$
$$\ldots - c_{M_{Z,yaw}} DR_{M_{Z,yaw},i} - 3c_{M_{Y,blade}} DR_{M_{Y,blade},i}\},$$
$$i \in \{-1,0,1\}, \tag{10}$$

where DR_{YM_y} and DR_{YM_z} are damage rates of the yaw bearing caused by M_y and M_z loadings, whereas DR_{BM_y} is the damage rate experienced by the blade root due to M_y loading and index i denotes the operating condition of the yaw control system. The performance functions are stored in a form of 2-dimensional look-up tables for the operation of the optimal wind turbine yaw controller. Since yaw misalignment Ψ equals $\angle V_w - \gamma$, performance function F_i (10) is in the considered case a function of the wind nacelle orientation and wind speed disturbance variable, $F_i = f(\gamma, d)$.

C. Optimisation approach

Employing the identified performance functions and the dynamical model of yawing, it is possible to pose the optimal wind turbine yaw control problem. For the nacelle performing a manoeuvre (see Fig. 9) each discrete-time step of the low level control system consists of maximally two nacelle states, rotation and holding position.

Each of the nacelle states should be represented with an adequate measure of the performance function. While on the one side holding position is clearly quantified from the static performance function data with respect to the constant wind speed value and misalignment, the overall performance during the nacelle rotation is an integral measure

$$J_{k,rotation} = \int_0^{w_{k,1} T_d} F_*(\gamma(\tau), d_k) d\tau. \tag{11}$$

where the asterisk mark $*$ denotes either the maximum negative -1 or positive 1 rotating states. Low enough discretisation time of the high level control system allows one to assume F_*

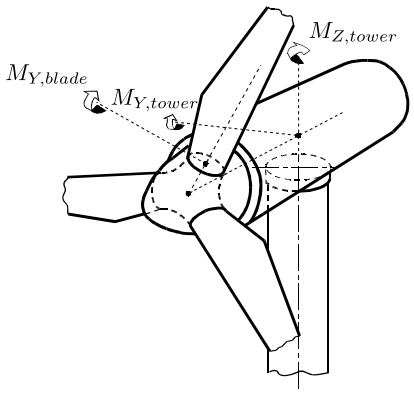

Fig. 5. GH Bladed coordinate systems for most significant loads [17] for the considered wind turbine

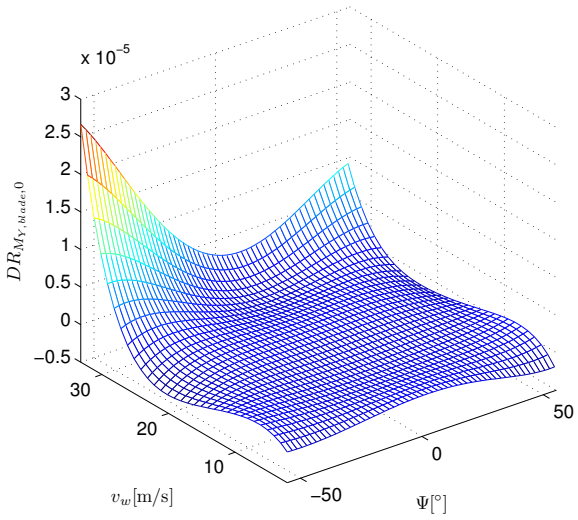

Fig. 6. Damage rate due to the blade bending torque M_y for fixed nacelle

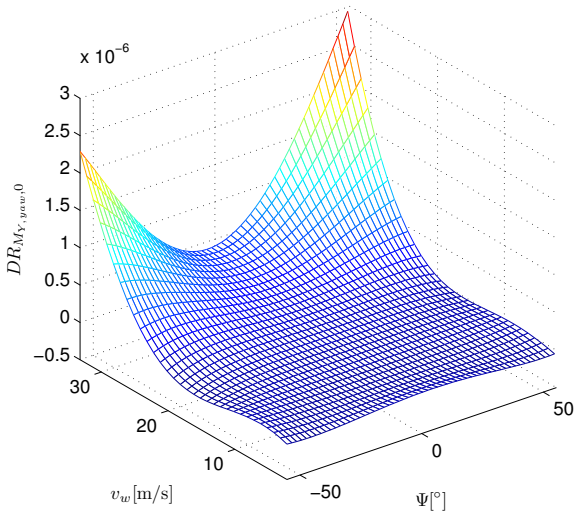

Fig. 7. Damage rate due to the yaw bending torque M_y for fixed nacelle

to be approximately affine with respect to the active domain in the rotation interval. This assumption allows one to use the following averaged performance function instead of the continuous integral (11)

$$J_{k,rotation} \approx w_{k,1} T_d F_*(\gamma_k + \frac{\omega_y T_d u_k}{2}, d_k). \qquad (12)$$

Hence, the overall performance function for one discrete-

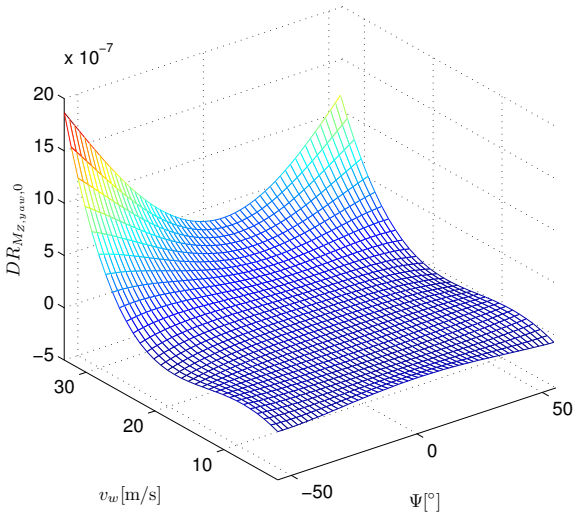

Fig. 8. Damage rate due to the yaw twisting torque M_z for fixed nacelle

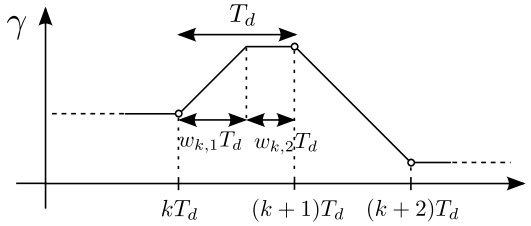

Fig. 9. Illustration of active $w_{k,1}$ and inactive $w_{k,2}$ time interval during the yaw manoeuvre

time interval is

$$J_k(u_k, \gamma_k, d_k) = \begin{cases} w_{k,1} F_{-1}(\gamma_k + \frac{\omega_y T_d u_k}{2}, d_k) + \dots \\ \dots + w_{k,2} F_0(\gamma_k + \omega_y T_d u_k, d_k), \; u \le 0, \\ w_{k,1} F_1(\gamma_k + \frac{\omega_y T_d u_k}{2}, d_k) + \dots \\ \dots + w_{k,2} F_0(\gamma_k + \omega_y T_d u_k, d_k), \; u > 0, \end{cases} \qquad (13)$$

$$w_1 = |u|, \; w_2 = 1 - |u|,$$

where $w_{k,1}$ and $w_{k,2}$ are the relative lengths of the active and inactive yaw system rotation intervals in the discrete-time step k, respectively. Performance function (13) is nonlinear and non-convex what means that optimality guarantees can not be provided. There are various approaches to yield suboptimal solution for the respective class of problems, whereas gradient based optimization method is used in this article to perform the control performance optimisation. The starting optimal control problem

$$U^* = \arg\max_U \sum_k J_k(u_k, \gamma_k, d_k)$$
$$\text{s.t.} \quad \left.\begin{matrix} u_k \in (-1, 1) \\ -4\pi \le \gamma_{k+1} \le 4\pi \end{matrix}\right\} \forall k \in \{0, 1, \dots, N-1\}, \qquad (14)$$

is divided into smaller subproblems which can be efficiently solved. Gradient-based optimization method is performed in iterative manner, employing successively linearised performance function and imposed bounds on the control inputs,

$$\left.\frac{\partial J}{\partial \Delta U}\right|_{U_0} = [1,\ldots,1]\cdot\begin{bmatrix} \frac{\partial J_0}{\partial \Delta u_0} & 0 & 0\ldots & 0 \\ \frac{\partial J_1}{\partial \Delta u_0} & \frac{\partial J_1}{\partial \Delta u_1} & 0\ldots & 0 \\ \vdots & \ddots & \ddots & \vdots \\ \frac{\partial J_{N-1}}{\partial \Delta u_0} & \frac{\partial J_{N-1}}{\partial \Delta u_1} & \cdots & \frac{\partial J_{N-1}}{\partial \Delta u_{N-1}} \end{bmatrix},$$
$$\Delta U \geq k_l,\ \Delta U \leq k_r, \tag{15}$$

where $\Delta U \in \mathbb{R}^N$ is the optimization vector deviation around the linearisation point U_0, k_l and k_r are allowed lower and upper perturbation bounds, respectively. Gradient based method ensures convergence to the closest local maximum with maximum convergence rate specified with the perturbation bounds. Gradient method is stopped when specified limit on the number of iterations is reached or after the improvement of the performance function between the successive iterations drops below the specified tolerance limit. For the gradient-based optimization method, it is of high importance to find initial optimization vector that is close to the optimal solution.

With respect to the nature of the considered problem, we propose to initialize the optimization vector with respect to the solution of the following quadratic program

$$\begin{aligned} U^*_{init} = \quad & \arg\min_{U} \sum_k \left(\Psi_k - \Psi_{opt,k}\right)^2, \\ & \text{s.t.} \quad u_{init,k} \in (-1,1) \end{aligned} \tag{16}$$

where the optimal angle of yaw misalignment Ψ_{opt} is determined with respect to the predicted wind speed values for fixed wind turbine nacelle $J(0, x_k, d_k)$. Note that for the real-time optimization of (16), code generated using the FiOrdOs Matlab toolbox for solving parametric convex optimization problems is employed [18]. Initial optimization vector U^*_{init} is passed to the gradient-based optimiser.

V. Simulation Results

In order to perform a quantitative comparison of the optimal yaw controller performance with respect to the baseline yaw control system, 10 wind fields with different mean wind speed and duration equal to 120 [min] are generated. Wind fields cover all operating region of the wind turbine what allows a life-time analysis of the extracted wind energy and experienced damage equivalent loads. Obtained results of DELs reduction experienced with the optimal yaw control system with respect to the baseline control system are shown in Figs. 10 and 11. It has to be noted that the baseline controller operates incorporating persistent model for the wind predictions, while optimal controller employs 20 [min] long wind predictions. Uncertainty of the predictions utilized by the optimal controller is modelled with an additive white Gaussian noise, incorporating 25 % lower standard deviation of the prediction errors compared to the persistent prediction model. Time responses of the selected control system variables are shown in Fig. 12. Shown simulation results demonstrate the

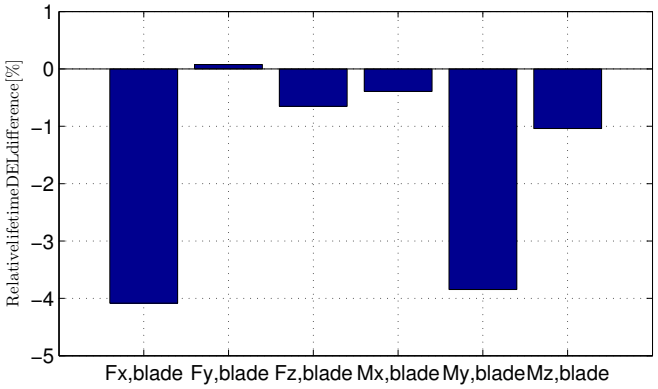

Fig. 10. Relative measures of the life-time blade DELs comparing the optimal controller to the baseline

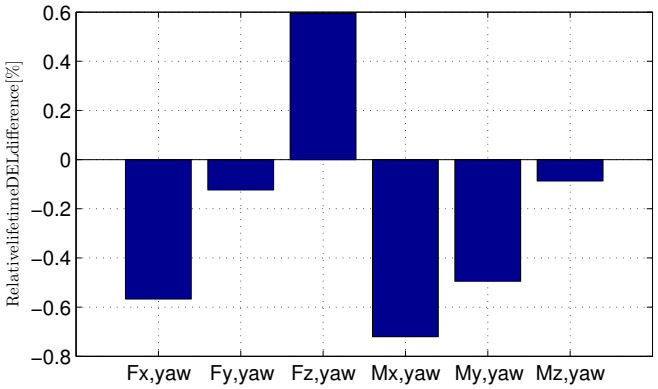

Fig. 11. Relative measures of the life-time yaw bearing DELs comparing the optimal controller to the baseline

effectiveness of the applied optimal yaw controller compared to the baseline control system with respect to reduced DELs. From the power production point of view, life-time analysis showed power production increase of ≈ 0.6 %, owing to the optimal yaw controller.

Optimal controller performs better for several reasons. First of all, wind velocity prediction allows the controller to react proactively in order to reduce the cumulative yaw misalignment. Moreover, optimal controller exploits model of experienced damage for selected wind turbine components with respect to various wind conditions and consequently positions the yaw misalignment at the optimal angle which is not always equal to zero.

VI. Conclusion

This paper describes the design of the optimal wind turbine yaw controller that exploits information about the wind velocity prediction in order to compute the optimal control policy. Optimal yaw control problem is formulated to include all relevant indicators for the successful operation of the wind turbine. Arising optimal control problem is solved in a suboptimal way that is practical and implementable on the real wind turbine hardware.

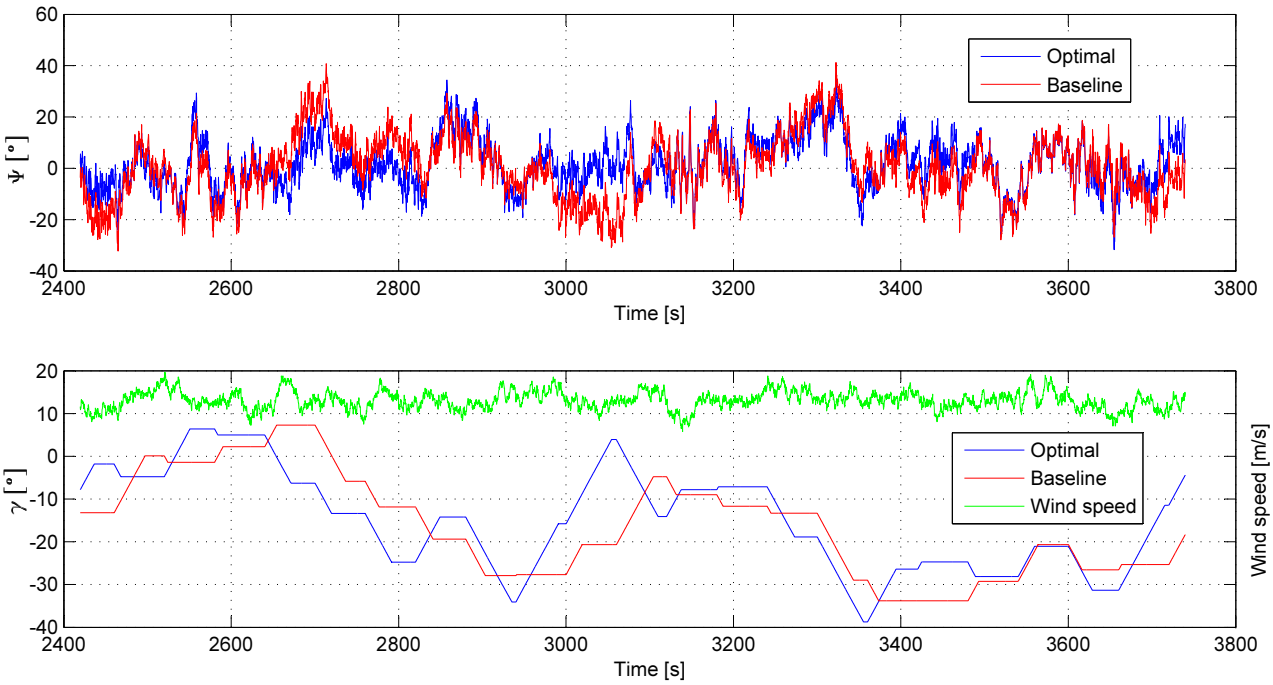

Fig. 12. Time response of the yaw misalignment (upper subfigure) and measured nacelle angle (lower subfigure) for the baseline and optimal control system

Performance of designed optimal yaw controller is compared to the baseline control system performance employing GH Bladed simulation tool. The results show superiority of the optimal yaw controller compared to the baseline with respect to the damage equivalent loads reduction in the wind turbine blade root and yaw bearing as well as in the power production increase. Designed optimal yaw controller showed to perform worse only with respect to the damage equivalent loads due to the blade loads $F_{Y,blade}$ and yaw bearing loads $F_{Z,yaw}$. While the damage equivalent loads increase which is experienced in the blade root is statistically insignificant, damage equivalent loads increase due to the $F_{Z,yaw}$ loads is solely a consequence of the more upright wind turbine position during the optimal yaw controller operation.

In the following research, point-wise load analysis of the wind turbine components will be substituted with component-wise load analysis for the yaw drive, blade and tower. Moreover, the average wind direction and wind speed change will be generated according to the more realistic model, possibly exploiting available real field data.

ACKNOWLEDGMENT

This work has been financially supported by the European Union through project CEEStructHealth - Centre of Excellence for Structural Health, grant No. IPA2007/HR/16IPO/001-040513.

REFERENCES

[1] T. W. W. E. Association, "2014 half year report," Bonn, Germany, Tech. Rep., 2014.

[2] F. Chen and J. Yang, "Fuzzy pid controller used in yaw system of wind turbine," in *Power Electronics Systems and Applications, 2009. PESA 2009. 3rd International Conference on*, May 2009, pp. 1–4.

[3] F. Farret, L. Pfitscher, and D. Bernardon, "Sensorless active yaw control for wind turbines," in *Industrial Electronics Society, 2001. IECON '01. The 27th Annual Conference of the IEEE*, vol. 2, 2001, pp. 1370–1375 vol.2.

[4] M. Liao, L. Dong, L. Jin, and S. Wang, "Study on rotational speed feedback torque control for wind turbine generator system," in *Energy and Environment Technology, 2009. ICEET '09. International Conference on*, vol. 1, Oct 2009, pp. 853–856.

[5] K. Wu, R. Joseph, and N. Thupili, "Evaluation of classical and fuzzy logic controllers for wind turbine yaw control," in *Aerospace Control Systems, 1993. Proceedings. The First IEEE Regional Conference on*, May 1993, pp. 254–258.

[6] F. Farret, L. Pfischer, and D. Bernardon, "Active yaw control with sensorless wind speed and direction measurements for horizontal axis wind turbines," in *Devices, Circuits and Systems, 2000. Proceedings of the 2000 Third IEEE International Caracas Conference on*, 2000, pp. I25/1–I25/6.

[7] W. Xin, L. Yanping, and T. Wei, "Modified hill climbing method for active yaw control in wind turbine," in *Control Conference (CCC), 2012 31st Chinese*, July 2012, pp. 6677–6680.

[8] S. S. Soman, H. Zareipour, O. Malik, and P. Mandal, "A review of wind power and wind speed forecasting methods with different time horizons," in *North American Power Symposium (NAPS), 2010*. IEEE, 2010, pp. 1–8.

[9] S. Pourmousavi Kani and M. Ardehali, "Very short-term wind speed prediction: a new artificial neural network–markov chain model," *Energy Conversion and Management*, vol. 52, no. 1, pp. 738–745, 2011.

[10] M. Djalto, M. Vašak, M. Baotić, J. Matuško, and K. Horvath, "Neural-network-based ultra-short-term wind forecasting," in *EWEA 2014 Annual Event*, 2014.

[11] G. Hayman, "Mlife theory manual for version 1.00," *National Renewable Energy Laboratory (NREL) Golden, CO*, 2012.

[12] E. F. Camacho and C. B. Alba, *Model predictive control*. Springer, 2013.

[13] A. Bamimore, O. Taiwo, and R. King, "Comparison of two nonlinear model predictive control methods and implementation on a laboratory three tank system," in *Decision and Control and European Control Conference (CDC-ECC), 2011 50th IEEE Conference on*, Dec 2011, pp. 5242–5247.

[14] J. Mu and D. Rees, "Approximate model predictive control for gas turbine engines," in *American Control Conference, 2004. Proceedings of the 2004*, vol. 6, June 2004, pp. 5704–5709 vol.6.

[15] F. Oldewurtel, C. Jones, A. Parisio, and M. Morari, "Stochastic model predictive control for building climate control," *Control Systems Technology, IEEE Transactions on*, vol. 22, no. 3, pp. 1198–1205, May 2014.

[16] International standard, "Wind turbines - part 1: Design requirements, IEC 61400-1, ed. 3,," 2005.

[17] E. Bossanyi, "Gh bladed user manual," *Garrad Hassan Bladed*, 2009.

[18] F. Ullmann, "A matlab toolbox for c-code generation for first order methods," Master's thesis, ETH Zurich.